The relationship between liquid, supercooled and glassy water

Osamu Mishima & H. Eugene Stanley

That water can exist in two distinct 'glassy' forms—low- and high-density amorphous ice—may provide the key to understanding some of the puzzling characteristics of cold and supercooled water, of which the glassy solids are more-viscous counterparts. Recent experimental and theoretical studies of both liquid and glassy water are now starting to offer the prospect of a coherent picture of the unusual properties of this ubiquitous substance.

At least one 'mysterious' property of liquid water seems to have been recognized 300 years ago[1]: whereas most liquids contract as temperature decreases, liquid water begins to expand when its temperature drops below 4 °C. A kitchen experiment demonstrates that the bottom layer of a glass of unstirred iced water remains at 4 °C while colder layers 'float' on top; the temperature at the bottom rises only after all the ice has melted.

The mysterious properties of liquid water become more pronounced in the supercooled region below 0 °C (refs 2–4; Fig. 1). For example, if the coefficient of thermal expansion, isothermal compressibility, and constant-pressure specific heat are extrapolated below the lowest temperatures at which these properties are measurable (about −38 °C at 1 bar) they appear to become infinite at an unreachable temperature $T_s \approx -45$ °C (refs 2, 5), at which point the entire concept of a 'liquid state' becomes difficult to sustain.

Water is a liquid, but glassy water—also called amorphous ice—can exist when the temperature drops below the glass transition temperature T_g (about 130 K at 1 bar). Although glassy water is a solid, its structure exhibits a disordered liquid-like arrangement. Low-density amorphous ice (LDA) has been known to exist for 60 years (ref. 6), and a second kind of amorphous ice, high-density amorphous ice (HDA), was discovered in 1984[7–9]. Thus ice has two different amorphous forms. This phenomenon is called polyamorphism, a term meaning that the pure material can exist in more than one amorphous state[10,11]. All amorphous solid forms of H_2O can be partitioned into these two low-density and high-

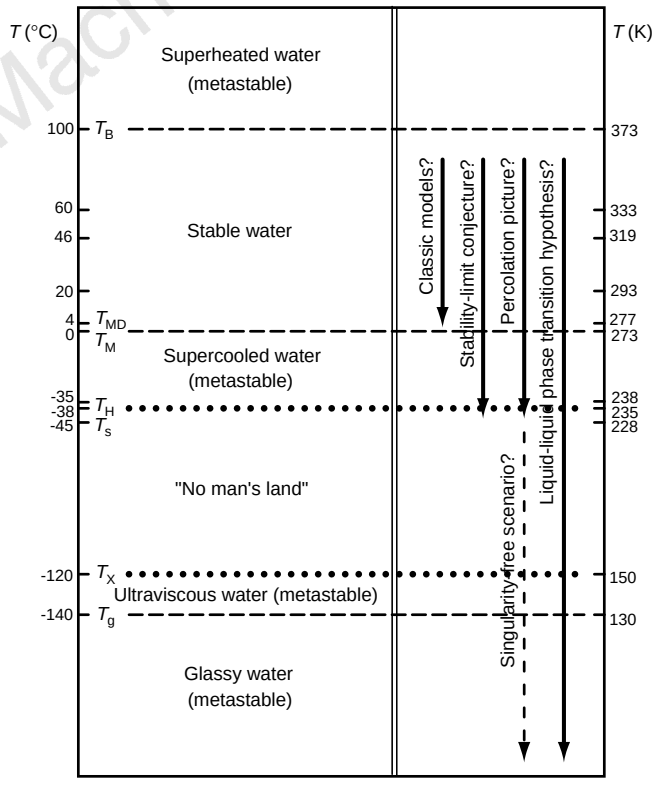

Figure 1 Schematic illustration of different temperature domains, at atmospheric pressure, of H_2O. One domain is stable; the others are metastable. Indicated on the right side of the diagram are the approximate temperature domains which proposed explanations are intended to describe. All the indicated numbers are experimentally observed (and are defined in the text), except the number denoted T_s (about –45 °C) which is a fitting parameter that emerges from assuming the existence of a power-law singularity in measured thermodynamic response functions. The region between the homogeneous nucleation curve $T_H(P)$ and the crystallization curve $T_X(P)$ is a kind of 'no-man's-land', as experiments on the liquid phase cannot be performed. The temperatures denoted 60 °C, 46 °C, 20 °C and 4 °C indicate the onset of anomalies in the sound velocity, isothermal compressibility, shear viscosity, and density, respectively[2,3]. T_{MD} denotes the temperature of maximum density, T_B the boiling temperature, T_M the melting temperature, and T_g the glass transition temperature.

density forms, although there may be slight variations in the individual structures depending on the preparation method and procedure[12–15].

LDA was originally produced by depositing water vapour onto a cold plate[6] or by cooling micrometre-sized droplets of liquid water extremely rapidly[12,16,17]. It was once believed that LDA could be nanocrystalline because of its structural resemblance to the most common form of ice, ice I_h (ref. 18). Now it is agreed that LDA is amorphous, as it transforms to a highly viscous liquid[19] when heated to the known glass transition temperature of about 130 K (refs 20–22).

In contrast, HDA was discovered by compressing ice I_h below a temperature of about 150 K (refs 7, 13, 23). HDA was independently discovered by bombarding an ice-I_h layer with an electron beam[8,24]. The transformation from a crystalline phase to a (presumably metastable) amorphous phase is called amorphization[25,26] (Fig. 2). When compressed further at low enough temperatures, HDA crystallizes and becomes a high-density crystalline ice[23,27].

In addition to the original preparation methods from the vapour, liquid or crystalline phases of water, LDA can be formed directly from HDA—and vice versa (Fig. 2). This 'polyamorphic transition' is accompanied by a surprisingly sharp and surprisingly large volume change—more than 20%—when thermodynamic parameters such as temperature or pressure change infinitesimally. The properties of the amorphous ices change apparently discontinuously at the polyamorphic transition. For example, the shear modulus of LDA decreases on compression, jumps discontinuously at the LDA → HDA transition, and then increases with further compression[28]. Therefore, the transformation between LDA and HDA appears to be a first-order transition between two different metastable amorphous 'phases', rather than a relaxation phenomenon in which an unstable amorphous structure changes continuously from LDA to HDA. Simulations also reveal such polyamorphic transitions[27,29].

HDA has a structure similar to that of high-pressure liquid water, suggesting that HDA is a glassy form of high-pressure water[30–32]. Thus far, however, the glass transition of HDA has not been observed.

There is a continuing discussion about whether pressure-induced amorphization[13,26,33,34] is conventional 'two-phase melting' (crystalline solid becoming liquid) at a temperature below T_g, or is what is called 'one-phase melting' (a collapse transition—solid becoming collapsed solid)[35] (Fig. 3). Thus it remains unresolved whether one considers HDA to be a glassy state of liquid water or to be a collapsed 'ill-crystalline' phase. Regarding HDA as a glass of a high-pressure liquid, Whalley *et al.*[36] predicted from thermodynamic arguments the location of the low-temperature metastable melting line of ice I_h—a prediction later confirmed by experiments[13]—which located the ice I_h melting line above the supposed glass transition temperature T_g. Below T_g, amorphization does not occur on the extrapolation of the two-phase melting line, as once believed[37], but rather melting is 'delayed' to higher pressures[13] as suggested in ref. 36 (Fig. 3). This delayed melting can be interpreted as a shift from two-phase melting to one-phase melting.

Here we discuss the status of experimental knowledge of liquid and glassy water in the light of recent theoretical attempts to obtain a unified picture of the liquid, supercooled and glassy states and the transformations between them. These theoretical proposals typically focus on the thermodynamic anomalies exhibited by supercooled water, offering explanations for the singularity-like behaviour that seems to occur at about −45 °C. However, it has proved very difficult to find discriminating experimental tests that will allow the theoretical models to be evaluated, and the matter is still unresolved. Computer simulations are unable to resolve the issue either, because water is notoriously hard to simulate realistically and the results can be highly sensitive to the intermolecular potential functions used. Nonetheless, we hope to show that the picture is now becoming clearer, in that some experiments do seem to lend support to specific theoretical models, while simulations have elucidated interrelationships between them. In particular, we can start to discern the origins of water's anomalous behaviour within the nature of its intermolecular forces. The prospect of a unified picture of water now seems to be in view.

Hypotheses

Many classic 'explanations' for the mysterious behaviour of liquid water have been developed[38–42], including a simple two-state model dating back to Röntgen[43] and a clathrate model dating back to Pauling[44]. Here we shall briefly describe three relatively recent hypotheses under active current discussion.

One of the popular explanations is the stability limit hypothesis[45], which assumes that the spinodal temperature line $T_s(P)$ in the pressure–temperature (P–T) phase diagram connects at negative P to the locus of the liquid-to-gas spinodal (the limit of metastability) for superheated water (Fig. 4a). It is assumed that liquid water cannot exist when cooled or stretched beyond the line $T_s(P)$.

The data supporting the singularity at T_s are limited to temperatures several degrees above T_s. Hence it is possible that functions have a rapid rise but that there is no singularity, behaviour predicted

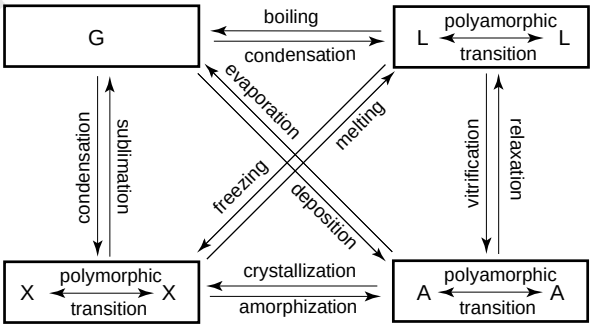

Figure 2 Transitions between gas (G), liquid (L), crystal (X) and amorphous (A) phases of water. We note that the amorphous 'phase' is metastable and non-ergodic (meaning a non-equilibrium state in a metastable phase), so the three transitions to and from 'A' are different from the other transitions because 'A' has many local minima; thus these transitions are not true thermodynamic transitions, but rather depend upon the timescale and other experimental conditions. The transitions to and from 'A'–and the transitions to and from 'X'–must be distinguished from those coming from polymorphism and polyamorphism.

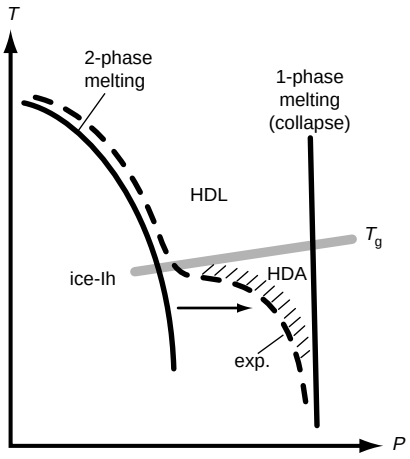

Figure 3 Two-phase melting contrasted with one-phase melting. T–P phase diagram showing the shift of the melting line $T_M(P)$ of ice I_h from 'two-phase melting' above T_g to 'one-phase melting' below T_g. The experimental data, marked 'exp.', follow the dashed line.

by the percolation hypothesis which treats water as a locally structured transient gel comprised of monomers—water molecules—held together by hydrogen bonds whose number increases as temperature decreases[46]. The local 'patches' or bonded subdomains[47] lead to enhanced fluctuations of specific volume and entropy, and to negative cross-correlations of volume and entropy whose anomalies closely match those observed experimentally. The percolation hypothesis has been recognized to be only one example of a more general framework, termed the singularity-free hypothesis (Fig. 4b), that considers the possibility that the observed polyamorphic changes in water are essentially relaxation phenomena that resemble a genuine transition, but are not[48].

A third recent proposal to rationalize the mysterious properties of water is called the liquid–liquid phase-transition hypothesis (Fig. 4c), which arose from molecular dynamics studies on the structure and equation of state of supercooled water[49] and has received support from various theoretical approaches[50–54]. Below the known critical point—with coordinates $T_c = 647\,\mathrm{K}$, $P_c = 22\,\mathrm{MPa}$ and critical density $\rho_c = 0.328\,\mathrm{g\,cm^{-3}}$—the high-pressure and high-temperature fluid phase separates into two distinct fluid phases: a low-density gas phase at low pressure and a higher-density liquid phase at high pressure. Below the hypothesized second critical point—with coordinates $T_{c'} \approx 220\,\mathrm{K}$, $P_{c'} \approx 100\,\mathrm{MPa}$ and $\rho_{c'} \approx 1\,\mathrm{g\,cm^{-3}}$—the liquid phase separates into two distinct liquid phases: a low-density liquid (LDL) phase at low pressures and a high-density liquid (HDL) at high pressure (Fig. 5a). Water near the known critical point is a fluctuating mixture of molecules whose local structures resemble the liquid and gas phases. Similarly, water near the hypothesized second critical point is a fluctuating mixture of molecules whose local structures resemble the two phases, LDL and HDL. These enhanced fluctuations influence the properties of liquid water, thereby leading to anomalous behaviour.

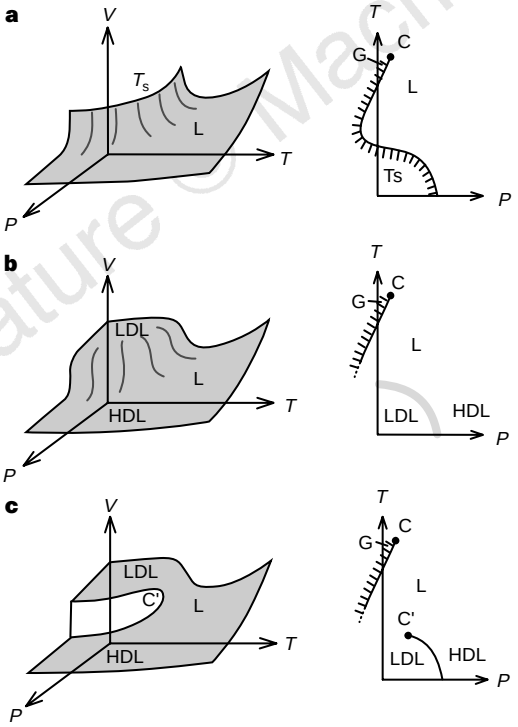

Figure 4 Thermodynamic behaviour of water predicted by three competing theories. The $V(P, T)$ equilibrium equation-of-state surface (left panels) and the projection onto the P–T plane (right panels) for **a**, the stability limit hypothesis, **b**, the percolation picture (and singularity-free hypothesis), and **c**, the liquid–liquid phase-transition hypothesis. Here C denotes the known critical point, C′ indicates the hypothesized second critical point, and $T_s(P)$ shows the locus of spinodal temperatures. G and L denote the low-density and high-density fluid phases that exist below C, while LDL and HDL denote the low-density and high-density liquid phases that exist below C′.

Experimental results

Many precise experiments have been performed to test the various hypotheses discussed above, but there is as yet no widespread agreement on which physical picture—if any—is correct. The connection between liquid water and the two amorphous ices predicted by the liquid–liquid phase-transition hypothesis is difficult to prove experimentally because supercooled water freezes spontaneously below the homogeneous nucleation temperature T_H, and amorphous ice crystallizes above the crystallization temperature T_X (refs 55–57). Freezing makes experimentation on the supercooled liquid state between T_H and T_X almost impossible. However, comparing experimental data on amorphous ice at low temperatures with that of liquid water at higher temperatures allows

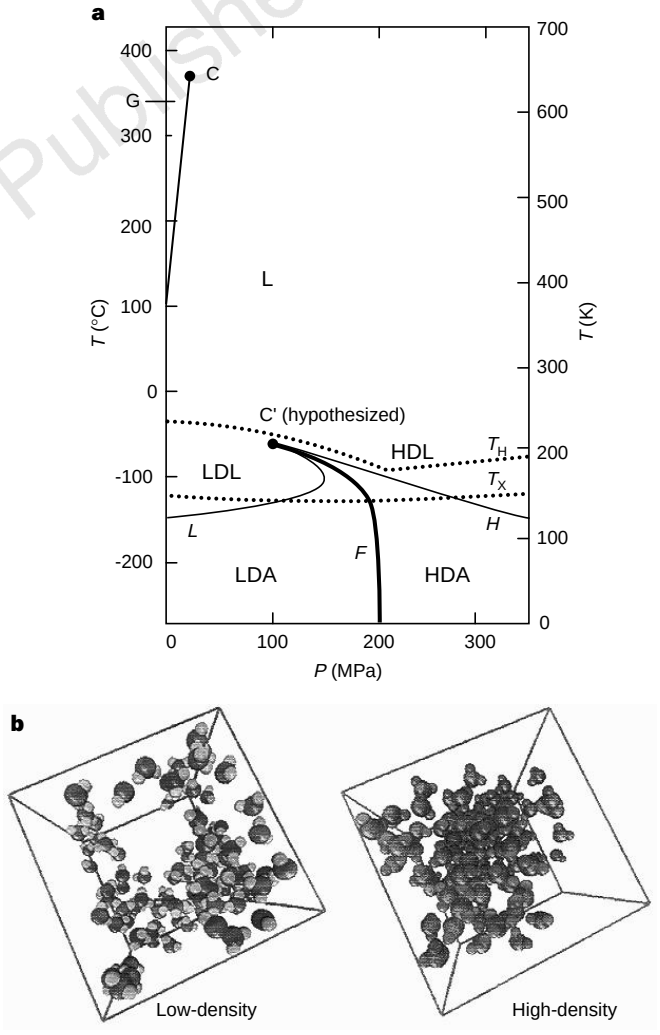

Figure 5 Detailed version of the projection onto the P–T plane of the equilibrium $V = V(P, T)$ surface of Fig. 4c. **a**, The phase relations between liquid water, LDL, HDL, LDA and HDA: C and C′ denote the known critical point and the hypothesized 'second' critical points respectively, F denotes the line of first-order phase transitions that emanates from C′ and separates the high-density and low-density phases that occur for temperatures below $T_{c'}$. The curves denoted L and H are the limits of metastability of the HDA and LDA phases, respectively. **b**, Molecular-dynamics 'snapshots' of LDL and HDL, coexisting and separating in liquid water. The subset of water molecules identified in the left panel have a smaller local density than the average, while those shown in the right panel have a larger local density. Courtesy of S. Harrington.

an indirect discussion of the relationship between the liquid and amorphous states. It is found from neutron diffraction studies[30] and simulations[32] that the structure of liquid water changes towards the LDA structure when the liquid is cooled at low pressures, and changes towards the HDA structure when cooled at high pressures, which is consistent with the liquid–liquid phase-transition hypothesis[30,32]. The amorphous states (LDA and HDA) are at present considered to be 'smoothly' connected thermodynamically to the liquid state if the entropies of the amorphous states are small[36,58], and experimental results suggest that their entropies are indeed small[59].

In principle, it is possible to investigate experimentally the liquid state in the region between T_H and T_X during the extremely short time interval before the liquid freezes to crystalline ice[13,57,60]. Because high-temperature liquid water becomes LDA without crystallization when it is cooled rapidly at a pressure of 1 bar (refs 12, 16), LDA appears to be directly related to liquid water. A possible connection between liquid water at high pressure and HDA can be seen when ice crystals are melted using pressure[13]. Other experimental results[57] on the high-pressure ices[42,61] that might demonstrate a liquid–liquid first-order transition in the region between T_H and T_X have been obtained; these suggest the location of the second critical point to be roughly 100 MPa and 220 K (Fig. 6).

These experimental results are consistent with an LDL–LDA connection at low pressure and an HDL–HDA connection at high pressure as temperature decreases, and clearly show an LDA–HDA transitions at still lower temperatures. They are therefore compatible with both the liquid–liquid first-order transition hypothesis and with the singularity-free hypothesis.

Results from simulations

Many simulation studies of water have been performed, but all are subject to the familiar charge that 'you get out what you put in'. Water is particularly difficult to simulate because it is a molecular liquid and there is at present no universally agreed precise yet tractable intermolecular potential. Nevertheless, there are some distinct advantages of simulations over experiments. Experiments cannot probe the 'no man's land' that arises from homogeneous nucleation phenomena (Fig. 1), but nucleation does not occur on the timescale of computer simulations. Hence simulations have the advantage that they can probe the structure and dynamics well below T_H. Of the three hypotheses discussed above, the liquid–liquid phase-transition hypothesis is best supported by simulations, some using the ST2 potential which exaggerates the real properties of water, and others using the SPC/E and TIP4P potentials which underestimate them[49,62–66]. The precise location of the second critical point is difficult to obtain because the continuation of the first-order line is a locus of maximum compressibility[62,63,65].

Further, computer simulations may be used to probe the local structure of water. At low temperatures, many water molecules appear to possess one of two principal local structures, one resembling LDA and the other HDA[29,49,64,67] (Fig. 5b). Experimental data can also be interpreted in terms of two distinct local structures[68,69].

The following three points seem to be consistent both with simulations and with experimental results. (1) Two 'local' structures—differing in local density—fluctuate dynamically in high-temperature liquid water, and separate gradually as temperature decreases. (2) At low enough temperatures, the liquid structure resembles more and more the structure of LDA and HDA, depending on the pressure. (3) At extremely low temperatures, LDL and HDL seem to transform, continuously, to LDA and HDA, and one can construct a physically plausible Gibbs-energy surface for water[57].

Physical arguments

A critical point appears if the pair potential between two particles of the system exhibits a minimum, and Fig. 7a sketches the potential of such an idealized system. At high temperature, the system's kinetic energy is so large that the potential well does not have an effect, and the system is in a single 'fluid' (or gas) phase. At low-enough

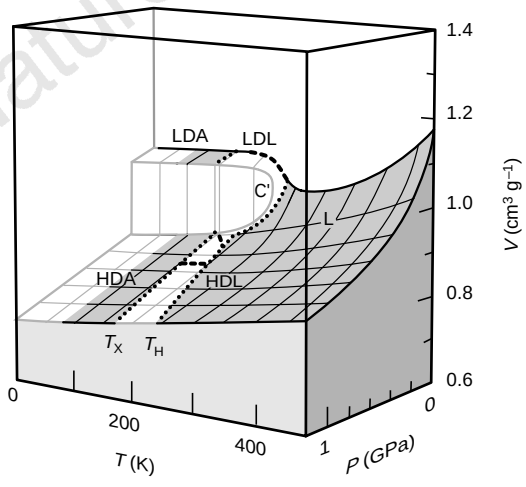

Figure 6 The pressure–volume–temperature relation for H_2O, on the basis of recent experiments[57]. The known LDA and HDA phases are shown, as well as the possible LDL and HDL phases hinted at by simulations[64] and the interpretation of experimental data[68]; the critical point, above which the LDL and HDL phases become indistinguishable, is also shown. The three dashed lines represent three 'bridges' across the 'no man's land' (white) separating the well-studied regions (grey), corresponding to the Mayer LDA experiment at $P = 1$ bar (ref. 12), and the melting lines of ice I_h (ref. 13) and ice XIV (ref. 57). C′ denotes the hypothesized LDL–HDL critical point.

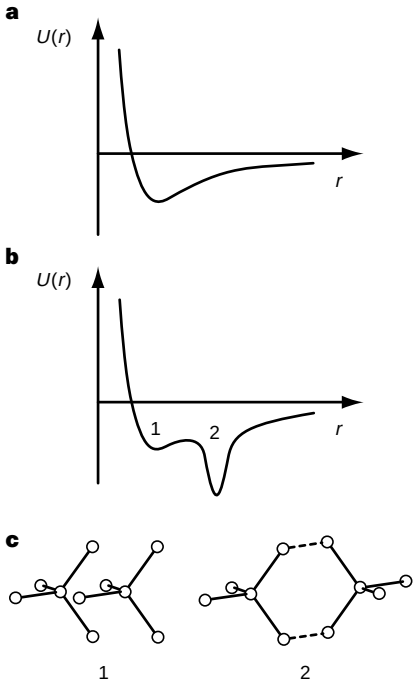

Figure 7 Physical arguments relating to the plausibility of the existence of the known liquid–gas critical point C and the hypothesized LDL–HDL critical point C′. **a**, Idealized system characterized by a pair interaction potential with a single attractive well. **b**, Idealized system characterized by a pair interaction potential whose attractive well has two sub-wells, the outer of which is deeper and narrower. **c**, Two idealized interaction clusters of water molecules in configurations that correspond to the two sub-wells of **b**.

temperature ($T < T_c$) and large-enough pressure ($P > P_c$), the fluid is sufficiently influenced by the minimum in the pair potential that it can condense into the low-specific-volume liquid phase. At lower pressure ($P < P_c$), the system explores the full range of distances—the large-specific-volume gas phase.

Suppose, now, that the potential well has the form shown in Fig. 7b—the attractive potential well shown in Fig. 7a has now bifurcated into a deeper narrow outer sub-well and a more shallow inner sub-well. Such a two-minimum potential can give rise to the occurrence at low temperatures of a second critical point. At high temperature, the system's kinetic energy is so large that the two sub-wells have no appreciable effect of the thermodynamics, and the liquid phase can sample both sub-wells. However, at low enough temperature ($T < T_{c'}$) and not too high a pressure ($P < P_{c'}$), the system must respect the depth of the outer sub-well so the liquid phase 'condenses' into the outer sub-well (the LDL phase). At higher pressure, it is forced into the shallower inner sub-well (the HDL phase). Thus there is a liquid–liquid phase transition at sufficiently low temperatures. It has been appreciated for some time[70,71] that one can obtain a liquid–liquid phase transition from potentials with generic features similar to the simplified potential shown in Fig. 7b.

The above arguments concern the average or 'thermodynamic' properties, but they may also be useful in anticipating the local properties in the neighbourhood of individual molecules. Consider, again, an idealized fluid with a potential of the form shown in Fig. 7a. Suppose that T is, say, 20% above T_c, so that the macroscopic liquid phase has not yet condensed out. Although the system is not entirely in the liquid state, small clusters of molecules begin to coalesce into the potential well, thereby changing their characteristic interparticle spacing (and hence their local specific volume) and their local entropy, so the fluid system will experience spatial fluctuations characteristic of the liquid phase even though this phase has not yet condensed out of the fluid at $T = 1.2\,T_c$. Specific-volume fluctuations are measured by the isothermal compressibility, and entropy fluctuations by the constant-pressure specific heat, so these two functions should start to increase from the values they would have if there were no potential well at all. As T decreases toward T_c, the magnitude of the fluctuations (and hence of the compressibility and the specific heat) increases monotonically and in fact diverges to infinity as $T \to T_c$. The cross-fluctuations of specific volume and entropy are proportional to the coefficient of thermal expansion, and this function should start to increase without limit as $T \to T_c$.

We now consider an idealized fluid with a potential of the form shown in Fig. 7b, and assume that T is below T_c but 20% above $T_{c'}$, so that the LDL phase has not yet condensed out. The liquid can nonetheless begin to sample the two sub-wells and clusters of molecules will begin to coalesce in each well, with the result that the liquid will experience spatial fluctuations characteristic of the LDL and HDL phase even though the liquid has not yet phase-separated. The specific-volume fluctuations and entropy fluctuations will increase, and so the isothermal compressibility and constant-pressure specific heat will start to diverge. Moreover, if the outer well is narrow, then when a cluster of neighbouring particles samples the outer well it has a larger specific volume and a smaller entropy, so the isothermal expansion coefficient (a measure of the cross-fluctuations of specific volume) is now negative, and approaches $-\infty$ as T decreases.

Now if by chance the value of $T_{c'}$ is lower than the value of T_H, then the actual phase separation discussed above can occur only at temperatures so low that the liquid would have frozen. In this case, the 'hint' of the second critical point is the presence of these local fluctuations whose magnitude would grow as T decreases, but which would never actually diverge if the second critical point is never in fact reached. Functions would be observed experimentally to increase as if they would diverge to ∞ or $-\infty$ but at a temperature below the range of experimental accessibility; we could not directly measure the phase separation itself.

Now consider not the above simplified potential, but rather the potential between water molecules. Presumably the attractive potential well of such a complex nonlinear molecule has structure, and presumably the tetrahedral nature of water dictates that the outermost well corresponds to the ordered configuration and hence has lower entropy. Thus although we do not know the actual form of the intermolecular potential in water, it is not implausible that the same considerations apply as those discussed for the simplified potential of Fig. 7b. Indeed, extensive studies of such pair potentials have been performed, and the existence of the second critical point has been demonstrated in such models[52,72–74].

To assess how plausible it is to obtain a bifurcated potential well of the form shown in Fig. 7b, we consider that water can be crudely approximated as a collection of five-molecule groups customarily called Walrafen pentamers (Fig. 7c)[69]. The interaction strengths of two adjacent Walrafen pentamers depends on their relative orientations. The first and the second energy minima of Fig. 7b correspond respectively to configurations 1 and 2 of adjacent Walrafen pentamers shown in Fig. 7c.

Configuration 1 in Fig. 7c is a high-energy, low-specific-volume, high-entropy, non-bonded state; configuration 2 in the same figure is a low-energy, high-specific-volume, low-entropy, bonded state. The difference in local structure between the two energy states depends on whether water molecules enter the empty space between the hydrogen bonds; this is also the difference in the local structure between a high-pressure crystalline ice (such as ice VI or ice VII) and a low-pressure crystalline ice (such as ice I_h)[42] (Fig. 7c).

The region of the P–T plane along the line continuing from the LDL–HDL coexistence line (when extrapolated to higher temperatures above the second critical point) is the locus of points where the LDL on the low-pressure side and the HDL on the high-pressure side are continuously transforming—it is called the line of compressibility maxima as it is the locus of points where the fluctuations in specific volume are largest. Near this line, two different kinds of

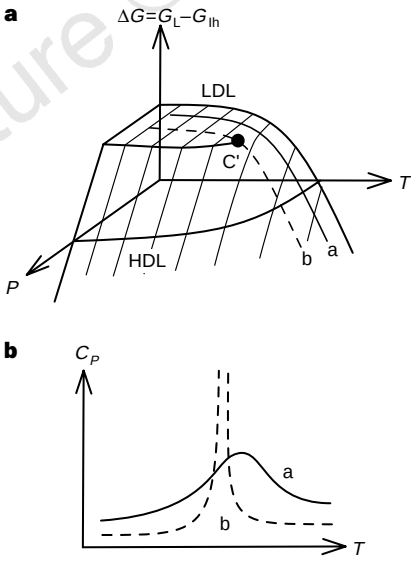

Figure 8 Effect of the hypothesized LDL–HDL critical point C′ on two constant-pressure paths, a and b, at pressures just below and just at the critical pressure of C′, respectively. **a**, Schematic of the Gibbs potential surface $G(P, T)$ for stable and metastable water, relative to that of ice I_h, predicted by the liquid–liquid phase-transition hypothesis. **b**, Prediction for the behaviour of the constant-pressure specific heat $C_P = -T(\partial^2 G/\partial T^2)_P$ at 1 atm pressure. As a well-defined line of C_P maxima must emanate from the second critical point, it follows that C_P must display a maximum along each subcritical isobar.

local structures, having either LDL or HDL properties, "coexist"[67,75,76]. The entropy fluctuations are also largest near this line and, as illustrated in Fig. 8, the constant-pressure specific heat C_P increases, displaying a lambda-like appearance[77]. Careful measurements and simulations of static and dynamic correlation functions[75,78–83] may be useful in determining the exact nature of the apparent singular behaviour near 220 K.

Possible implications

Possible forms of polyamorphism in condensed states have been reported, and several examples have been discussed[84]. In addition to H_2O (refs 9, 56, 85), polyamorphism has been studied in Si (ref. 86), and in Al_2O_3–Y_2O_3 (ref. 87). Liquids and amorphous solids that form network structures (like H_2O, SiO_2 (refs 88, 89), GeO_2 (refs 10, 90), C (refs 91, 92), and other III–V compounds[93]) are candidates for materials which show a polyamorphic transition and a second critical point. If, indeed, the molten states of SiO_2 and related minerals have polyamorphic transitions under high-pressure and high-temperature conditions inside the Earth, then the transitions may affect the early differentiation and geochemical evolution of this planet[94].

Which, if any, of the currently discussed hypotheses is correct could affect other fields of research in which water structure and dynamics are important. In chemistry, the structure and properties of aqueous solutions[95,96] might be viewed differently depending on which model is used. In biology, the correct hypothesis may affect the explanation of the structure and reaction of the liquid water around biological macromolecules[97]. Correct knowledge of the liquid state of water is also important for advancing the art of tissue cryopreservation[98]. Further, in chemical engineering, density and entropy fluctuations near the hypothesized second critical point might be important for aqueous reactions. The structure of water is of particular interest in confined systems[99], such as the clays that are of geological and biological interest. It has been speculated that polyamorphic transitions in liquid and amorphous solid water may occur inside (or on the surface of) icy bodies in space[24], and analogues of polyamorphic transitions have been proposed for the protein folding transition[100].

There are at least three contending hypotheses for rationalizing the puzzling features of liquid water. How to decide between these hypotheses is at a challenge to experimentalists and theoreticians alike, and the puzzling behaviour of liquid water is not yet resolved. Indeed, in the 300 years since the discovery of the density anomaly at 4 °C, many scientific puzzles have been solved, but the mystery of liquid water remains unsolved—despite the widespread importance of this substance. □

O. Mishima is at the National Institute for Research in Inorganic Materials (NIRIM), 1-1, Namiki, Tsukuba, Ibaraki 305-0044, Japan, and at Core Research for Evolutional Science and Technology (CREST), Japan Science and Technology Corporation (JST). H. E. Stanley is at the Center for Polymer Studies and Department of Physics, Boston University, Boston, Massachusetts 02215, USA.

1. Waller, R. (trans.) *Essays of Natural Experiments* (original in Italian by the Secretary of the Academie del Cimento); facsimile of the 1684 English translation (Johnson Reprint, New York, 1964).
2. Angell, C. A. in *Water: A Comprehensive Treatise* Vol. 7 (ed. Franks, F.) 1–81 (Plenum, New York, 1982).
3. Debenedetti, P. G. *Metastable Liquids* (Princeton Univ. Press, 1996).
4. Fourkas, J. T., Kivelson, D., Mohanty, U. & Nelson, K. A. (eds) *Supercooled Liquids: Advances and Novel Applications* (ACS Books, Washington DC, 1997).
5. Speedy, R. J. & Angell, C. A. Isothermal compressibility of supercooled water and evidence for a thermodynamic singularity at −45C. *J. Chem. Phys.* **65,** 851–858 (1976).
6. Burton, E. F. & Oliver, W. F. The crystal structure of ice at low temperatures. *Proc. R. Soc. Lond. A* **153,** 166–172 (1936).
7. Mishima, O., Calvert, L. D. & Whalley, E. 'Melting' ice I at 77 K and 10 kbar: a new method of making amorphous solids. *Nature* **310,** 393–395 (1984).
8. Heide, H.-G. Observations on ice layers. *Ultramicroscopy* **14,** 271–278 (1984).
9. Mishima, O., Calvert, L. D. & Whalley, E. An apparently first-order transition between two amorphous phases of ice induced by pressure. *Nature* **314,** 76–78 (1985).
10. Smith, K. H., Shero, E., Chizmeshya, A. & Wolf, G. H. The equation of state of polyamorphic germania glass: A two-domain description of the viscoelastic response. *J. Chem. Phys.* **102,** 6851–6857 (1995).
11. Poole, P. H., Grande, T., Sciortino, F., Stanley, H. E. & Angell, C. A. Amorphous polymorphism. *Comput. Mater. Sci.* **4,** 373–382 (1995).
12. Mayer, E. in *Hydrogen Bond Networks* (eds Bellissent-Funel, M.-C. & Dore, J. C.) 355–372 (Kluwer Academic, Dordrecht, 1994).
13. Mishima, O. Relationship between melting and amorphization of ice. *Nature* **384,** 546–549 (1996).
14. Johari, G. P., Hallbrucker, A. & Mayer, E. Two calorimetrically distinct states of liquid water below 150 Kelvin. *Science* **273,** 90–92 (1996).
15. Essmann, U. & Geiger, A. Molecular-dynamics simulation of vapor-deposited amorphous ice. *J. Chem. Phys.* **103,** 4678–4692 (1995).
16. Brüggeller, P. & Mayer, E. Complete vitrification in pure liquid water and dilute aqueous solutions. *Nature* **288,** 569–571 (1980).
17. Dubochet, J. & McDowall, W. A. Vitrification of pure water for electron microscopy. *J. Microsc.* **124,** RP3–RP4 (1981).
18. Blackman, M. & Lisgarten, N. D. The cubic and other structural forms of ice at low temperature and pressure. *Proc. R. Soc. Lond. A* **239,** 93–107 (1957).
19. Smith, R. S., Huang, C. & Kay, B. D. Evidence for molecular translational diffusion during the crystallization of amorphous solid water. *J. Phys. Chem. B* **101,** 6123–6126 (1997).
20. Sugisaki, M., Suga, H. & Seki, S. Calorimetric study of the glassy state. IV. Heat capacities of glassy water and cubic ice. *Bull. Chem. Soc. Jpn* **41,** 2591–2599 (1968).
21. McMillan, J. A. & Los, S. C. Vitreous ice: Irreversible transformations during warm-up. *Nature* **206,** 806–807 (1968).
22. Johari, G. P., Hallbrucker, A. & Mayer, E. The glass-liquid transition of hyperquenched water. *Nature* **330,** 552–553 (1987).
23. Hemley, R. J., Chen, L. C. & Mao, H. K. New transformations between crystalline and amorphous ice. *Nature* **338,** 638–640 (1989).
24. Jenniskens, P., Blake, D. F., Wilson, M. A. & Pohorille, A. High-density amorphous ice, the frost on interstellar grains. *Astrophys. J.* **455,** 389–401 (1995).
25. Johnson, W. L. Thermodynamic and kinetic aspects of the crystal to glass transformation in metallic materials. *Prog. Mater. Sci.* **30,** 81–134 (1986).
26. Sciortino, F. *et al.* Crystal stability limits at positive and negative pressures, and crystal-to-glass transitions. *Phys. Rev. E* **52,** 6484–6491 (1995).
27. Tse, J. S. & Klein, M. L. Pressure-induced phase transformations in ice. *Phys. Rev. Lett.* **58,** 1672–1675 (1987).
28. Brazhkin, V. V., Gromnitskaya, E. L., Stal'gorova, O. V. & Lyapin, A. G. Elastic softening of amorphous H_2O network prior to the *hda-lda* transition in amorphous state. *Rev. High Press. Sci. Technol.* **7,** 1129–1131 (1998).
29. Poole, P. H., Essmann, U., Sciortino, F. & Stanley, H. E. Phase diagram for amorphous solid water. *Phys. Rev. E* **48,** 4605–4610 (1993).
30. Bellissent-Funel, M. C. & Bosio, L. A neutron scattering study of liquid D_2O. *J. Chem. Phys.* **102,** 3727–3735 (1995).
31. Bellissent-Funel, M. C., Bosio, L., Hallbrucker, A., Mayer, E. & Sridi-Dorbez, R. X-ray and neutron scattering studies of the structure of hyperquenched glassy water. *J. Chem. Phys.* **97,** 1282–1286 (1992).
32. Starr, F. W., Bellissent-Funel, M.-C. & Stanley, H. E. Structural evidence for the continuity of liquid and glassy water. Preprint cond-mat/98111120 at <http://xxx.lanl.gov> (1998); also as *Proc. Les Houches School on Biological Aspects of Water* (ed. Bellissent, M.-C.) (Kluwer, Dordrecht, in the press).
33. Sharma, S. M. & Sikka, S. K. Pressure induced amorphization of materials. *Prog. Mater. Sci.* **40,** 1–77 (1996).
34. Ponyatovsky, E. G. & Barkalov, O. I. Pressure-induced amorphous phases. *Mater. Sci. Rep.* **8,** 147–191 (1992).
35. Tse, J. S. Mechanical instability in ice I_h: A mechanism for pressure-induced amorphization. *J. Chem. Phys.* **96,** 5482–5487 (1992).
36. Whalley, E., Klug, D. D. & Handa, Y. P. Entropy of amorphous ice. *Nature* **342,** 782–783 (1989).
37. Whalley, E., Mishima, O., Handa, Y. P. & Klug, D. D. Pressure melting below the glass transition: A new way of making amorphous solids. *Proc. NY Acad. Sci.* **484,** 81–95 (1986).
38. Bernal, J. D. & Fowler, R. H. A theory of water and ionic solution, with particular reference to hydrogen and hydroxyl ions. *J. Chem. Phys.* **1,** 515–548 (1933).
39. Pople, J. A. Molecular association in liquids. II. A theory of the structure of water. *Proc. R. Soc. Lond. A* **205,** 163–178 (1951).
40. Frank, H. S. & Wen, W.-Y. Structural aspects of ion-solvent interaction in aqueous solutions: A suggested picture of water structure. *Discuss. Faraday Soc.* **24,** 133–140 (1957).
41. Némethy, G. & Scheraga, H. A. Structure of water and hydrophobic bonding in proteins: I. A model for the thermodynamic properties of liquid water. *J. Chem. Phys.* **36,** 3382–3400 (1962).
42. Kamb, B. in *Structural Chemistry & Molecular Biology* (eds Rich, A. & Davidson, N.) 507–542 (Freeman, San Francisco, 1968).
43. Röntgen, W. C. Ueber die constitution des flüssigen wassers. *Ann. Phys. Chem.* **45,** 91–97 (1892).
44. Pauling, L. in *Hydrogen Bonding* (ed. Hadzi, D.) 1–5 (Pergamon, New York, 1959).
45. Speedy, R. J. Stability-limit conjecture. An interpretation of the properties of water. *J. Phys. Chem.* **86,** 982–991 (1982).
46. Stanley, H. E. & Teixeira, J. Interpretation of the unusual behavior of H_2O and D_2O at low temperatures: Tests of a percolation model. *J. Chem. Phys.* **73,** 3404–3422 (1980).
47. Geiger, A. & Stanley, H. E. Low-density patches in the hydrogen-bonded network of liquid water: Evidence from molecular dynamics computer simulations. *Phys. Rev. Lett.* **49,** 1749–1752 (1982).
48. Sastry, S., Debenedetti, P., Sciortino, F. & Stanley, H. E. Singularity-free interpretation of the thermodynamics of supercooled water. *Phys. Rev. E* **53,** 6144–6154 (1996).
49. Poole, P. H., Sciortino, F., Essmann, U. & Stanley, H. E. Phase behavior of metastable water. *Nature* **360,** 324–328 (1992).
50. Ponyatovskii, E. G., Sinitsyn, V. V. & Pozdnyakova, T. A. Second critical point and low-temperature anomalies in the physical properties of water. *JEPT Lett.* **60,** 360–364 (1994).
51. Moynihan, C. T. Two species/nonideal solution model for amorphous/amorphous phase transitions. *Mater. Res. Soc. Symp. Proc.* **455,** 411–425 (1997).
52. Poole, P. H., Sciortino, F., Grande, T., Stanley, H. E. & Angell, C. A. Effect of hydrogen bonds on the thermodynamic behavior of liquid water. *Phys. Rev. Lett.* **73,** 1632–1635 (1994).
53. Borick, S. S., Debenedetti, P. G. & Sastry, S. A lattice model of network-forming fluids with orientation-dependent bonding: equilibrium, stability, and implications from the phase behavior of supercooled water. *J. Phys. Chem.* **99,** 3781–3793 (1995).
54. Tejero, C. F. & Baus, M. Liquid polymorphism of simple fluids within a van der Waals theory. *Phys. Rev. E* **57,** 4821–4823 (1998).
55. Kanno, H., Speedy, R. & Angell, C. A. Supercooling of water to −92 °C under pressure. *Science* **189,** 880–881 (1975).
56. Mishima, O. Reversible first-order transition between two H_2O amorphs at ~0.2 GPa and ~135 K. *J. Chem. Phys.* **100,** 5910–5912 (1994).
57. Mishima, O. & Stanley, H. E. Decompression-induced melting of ice IV and the liquid-liquid transition in water. *Nature* **392,** 164–168 (1998).

58. Johari, G. P., Fleissner, G., Hallbrucker, A. & Mayer, E. Thermodynamic continuity between glassy and normal water. *J. Phys. Chem.* **98,** 4719–4725 (1994).
59. Speedy, R. J., Debenedetti, P. G., Smith, R. S., Huang, C. & Kay, B. D. The evaporation rate, free energy, and entropy of amorphous water at 150K. *J. Chem. Phys.* **105,** 240–244 (1996).
60. Bartell, L. S. & Huang, J. Supercooling of water below the anomalous range near 226 K. *J. Phys. Chem.* **98,** 7455–7457 (1994).
61. Bridgman, P. W. The pressure-volume-temperature relations of the liquid, and the phase diagram of heavy water. *J. Chem. Phys.* **3,** 597–605 (1935).
62. Poole, P. H., Sciortino, F., Essmann, U. & Stanley, H. E. The spinodal of liquid water. *Phys. Rev. E* **48,** 3799–3817 (1993).
63. Tanaka, H. Phase behaviors of supercooled water: Reconciling a critical point of amorphous ices with spinodal instability. *J. Chem. Phys.* **105,** 5099–5111 (1996).
64. Harrington, S., Zhang, R., Poole, P. H., Sciortino, F. & Stanley, H. E. Liquid-liquid phase transition: Evidence from simulations. *Phys. Rev. Lett.* **78,** 2409–2412 (1997).
65. Sciortino, F., Poole, P. H., Essmann, U. & Stanley, H. E. Line of compressibility maxima in the phase diagram of supercooled water. *Phys. Rev. E* **55,** 727–737 (1997).
66. Harrington, S., Poole, P. H., Sciortino, F. & Stanley, H. E. Equation of state of supercooled SPC/E water. *J. Chem. Phys.* **107,** 7443–7450 (1997).
67. Shiratani, E. & Sasai, M. Molecular scale precursor of the liquid-liquid phase transition of water. *J. Chem. Phys.* **108,** 3264–3276 (1998).
68. Bellissent-Funel, M.-C. Is there a liquid-liquid phase transition in supercooled water? *Europhys. Lett.* **42,** 161–166 (1998).
69. Canpolat, M. *et al.* Local structural heterogeneities in liquid water under pressure. *Chem. Phys. Lett.* **294,** 9–12 (1998).
70. Hemmer, P. C. & Stell, G. Fluids with several phase transitions. *Phys. Rev. Lett.* **24,** 1284–1287 (1970).
71. Sadr-Lahijany, M. R., Scala, A., Buldyrev, S. V. & Stanley, H. E. Liquid state anomalies for the Stell-Hemmer core-softened potential. *Phys. Rev. Lett.* **81,** 4895–4898 (1998).
72. Sastry, S., Sciortino, F. & Stanley, H. E. Limits of stability of the liquid phase in a lattice model with water-like properties. *J. Chem. Phys.* **98,** 9863–9872 (1993).
73. Roberts, C. J. & Debenedetti, P. G. Polyamorphism and density anomalies in network-forming fluids: Zeroth- and first-order approximations. *J. Chem. Phys.* **105,** 658–672 (1996).
74. Roberts, C. J., Panagiotopoulos, A. Z. & Debenedetti, P. G. Liquid-liquid immiscibility in pure fluids: Polyamorphism in simulations of a network-forming fluid. *Phys. Rev. Lett.* **77,** 4386–4389 (1996).
75. Shiratani, E. & Sasai, M. Growth and collapse of structural patterns in the hydrogen bond network in liquid water. *J. Chem. Phys.* **104,** 7671–7680 (1996).
76. Tanaka, H. Fluctuation of local order connectivity of water molecules in two phases of supercooled water. *Phys. Rev. Lett.* **80,** 113–116 (1998).
77. Angell, C. A., Shuppert, J. & Tucker, J. C. Anomalous properties of supercooled water. Heat capacity, expansivity, and proton magnetic resonance chemical shift from 0 to −38C. *J. Phys. Chem.* **77,** 3092–3099 (1973).
78. Sciortino, F., Fabbian, L., Chen, S.-H. & Tartaglia, P. Supercooled water and the kinetic glass transition: 2. Collective dynamics. *Phys. Rev. E* **56,** 5397–5404 (1997).
79. Sciortino, F., Gallo, P., Tartaglia, P. & Chen, S.-H. Supercooled water and the glass transition. *Phys. Rev. E* **54,** 6331–6343 (1996).
80. Xie, Y., Ludwig, K. F., Morales, G., Hare, D. E. & Sorensen, C. M. Noncritical behavior of density fluctuations in supercooled water. *Phys. Rev. Lett.* **71,** 2051–2053 (1993).
81. Sciortino, F., Poole, P. H., Stanley, H. E. & Havlin, S. Lifetime of the bond network and gel-like anomalies in supercooled water. *Phys. Rev. Lett.* **64,** 1686–1689 (1990).
82. Luzar, A. & Chandler, D. Hydrogen-bond kinetics in liquid water. *Nature* **379,** 55–57 (1996).
83. Starr, F. W., Nielsen, J. & Stanley, H. E. Fast and slow dynamics of hydrogen bonds in liquid water. Preprint cond-mat/9811120 at <http://xxx.lanl.gov> (1998); also as *Comput. Phys. Commun.* (in the press).
84. Brazhkin, V. V., Popova, S. V. & Voloshin, R. N. High-pressure transformations in simple melts. *High Press. Res.* **15,** 267–305 (1997).
85. Mishima, O., Takemura, K. & Aoki, K. Visual observations of the amorphous-amorphous transition in H_2O under pressure. *Science* **254,** 406–408 (1991).
86. Angell, C. A., Borick, S. & Grabow, M. Glass transitions and first order liquid-metal-to-semiconductor transitions in 4-5-6 covalent systems. *J. Non-cryst. Solids* **205,** 463–471 (1996).
87. Aasland, S. & McMillan, P. F. Density-driven liquid-liquid phase separation in the system Al_2O_3-Y_2O_3. *Nature* **369,** 633–636 (1994).
88. Grimsditch, M. Polymorhism in amorphous SiO_2. *Phys. Rev. Lett.* **52,** 2379–2381 (1984).
89. Poole, P. H., Hemmati, M. & Angell, C. A. Comparison of thermodynamic properties of simulated liquid silica and water. *Phys. Rev. Lett.* **79,** 2281–2284 (1997).
90. Itie, J. P. *et al.* Pressure-induced coordination changes in crystalline and vitreous GeO_2. *Phys. Rev. Lett.* **63,** 398–401 (1989).
91. Togaya, M. Pressure dependences of the melting temperature of graphite and the electrical resistivity of liquid carbon. *Phys. Rev. Lett.* **79,** 2474–2477 (1997).
92. Grumbach, M. P. & Martin, R. M. Phase diagram of carbon at high pressures and temperatures. *Phys. Rev. B* **54,** 15730–15741 (1996).
93. Ponyatovsky, E. G. & Pozdnyakova, T. A. The T-P phase diagrams of amorphous GaSb, InSb and InAs. *J. Non-cryst. Solids* **188,** 153–160 (1995).
94. Farber, D. L. & Williams, Q. Pressure-induced coordination changes in alkali-germinate melts: An in situ spectroscopic investigation. *Science* **256,** 1427–1430 (1992).
95. Angell, C. A. & Sare, E. J. Glass-forming composition regions and glass transition temperatures for aqueous electrolyte solutions. *J. Chem. Phys.* **52,** 1058–1068 (1970).
96. Leberman, R. & Soper, A. K. Effect of high salt concentrations on water structure. *Nature* **378,** 364–366 (1989).
97. Wiggins, P. M. Role of water in some biological processes. *Microbiol. Rev.* **54,** 432–449 (1990).
98. Dubochet, J. *et al.* Cryo-electron microscopy of vitrified specimens. *Q. Rev. Biophys.* **21,** 129–228 (1988).
99. Dore, J. in *Correlations and Connectivity* (eds Stanley, H. E. & Ostrowsky, N.) 188–197 (Kluwer Academic, Dordrecht, 1990).
100. Angell, C. A. Landscapes with megabasins: Polyamorphism in liquids and biopolymers and the role of nucleation in folding and folding diseases. *Physica D* **107,** 122–142 (1997).

Acknowledgements. We thank R. J. Hemley, H. Kanno, J. Karbowski, H. Kodama, E. La Nave, R. Sadr-Lahijany, S. Sastry, A. Scala, F. Sciortino, A. Skibinsky, F. W. Starr, Y. Suzuki and M. Yamada for discussions and critical reading of manuscript drafts. This work was supported by the NSF.

Correspondence and requests for materials should be addressed to H.E.S. (e-mail: hes@bu.edu) for theory, and O.M. at NIRIM (e-mail: mishima@ nirim.go.jp) for experiment.